

Simultaneous Automatic Picking and Manual Picking Refinement for First-Break

Haowen Bai, Zixiang Zhao, *Member, IEEE*, Jiangshe Zhang, Yukun Cui,
Chunxia Zhang, *Member, IEEE*, Zhenbo Guo, Yongjun Wang

Abstract—First-break picking is a pivotal procedure in processing microseismic data for geophysics and resource exploration. Recent advancements in deep learning have catalyzed the evolution of automated methods for identifying first-break. Nevertheless, the complexity of seismic data acquisition and the requirement for detailed, expert-driven labeling often result in outliers and potential mislabeling within manually labeled datasets. These issues can negatively affect the training of neural networks, necessitating algorithms that handle outliers or mislabeled data effectively. We introduce the Simultaneous Picking and Refinement (SPR) algorithm, designed to handle datasets plagued by outlier samples or even noisy labels. Unlike conventional approaches that regard manual picks as ground truth, our method treats the true first-break as a latent variable within a probabilistic model that includes a first-break labeling prior. SPR aims to uncover this variable, enabling dynamic adjustments and improved accuracy across the dataset. This strategy mitigates the impact of outliers or inaccuracies in manual labels. Intra-site picking experiments and cross-site generalization experiments on publicly available data confirm our method's performance in identifying first-break and its generalization across different sites. Additionally, our investigations into noisy signals and labels underscore SPR's resilience to both types of noise and its capability to refine misaligned manual annotations. Moreover, the flexibility of SPR, not being limited to any single network architecture, enhances its adaptability across various deep learning-based picking methods. Focusing on learning from data that may contain outliers or partial inaccuracies, SPR provides a robust solution to some of the principal obstacles in automatic first-break picking.

Index Terms—First-break picking, Microseismic signal, Outlier sample, Noisy label learning.

I. INTRODUCTION

FIRST-BREAK picking consists of identifying and recording the first arrival time of seismic energy at each receiver after a seismic event. This process is fundamental to seismic data analysis, offering insights into the locational aspects of seismic events and enabling the derivation of the seismic velocity structure within the Earth's subsurface. Its pivotal

role extends across a spectrum of geophysical explorations, encompassing both passive and active seismic methodologies. Notable applications include the monitoring of carbon capture and storage (CCS) [1], [2], underground hydrogen storage (UHS) [3], early warning of earthquakes, large-scale monitoring through distributed acoustic sensing (DAS) [4], [5], modeling of seismic velocities, analyzing geologic structures, and correction of the source/receiver coordinates. Given the extensive applications and the growing volume and complexity of seismic datasets, the pursuit of enhancing automatic first-break picking algorithms is increasingly pressing in the realm of seismic signal processing. These automatic algorithms are gradually replacing traditional manual picking, previously reliant on the expertise of seismologists. The transition is propelled by the advantages of automation, including efficiency, consistency, and accuracy. These qualities are becoming increasingly indispensable in the era of big data and with the advancement of high-resolution seismic imaging technologies.

Early traditional automatic techniques are characterized by the employment of statistical and signal processing algorithms such as energy-based methods [6]–[8], correlation-based methods and Akaike information criterion (AIC)-based methods. Short-term average/long-term average (STA/LTA) method [6], [7], [9]–[11] and its derivatives [12]–[20], as prominent energy-based methods, rely on the variation of energy ratio around the sample point to determine the time of first-break. Notably, utilizing multi-window energy ratios enables a more robust detection of first-break [14], [19]–[21]. Energy-based methods are straightforward and computationally inexpensive, and are less effective under low signal-to-noise conditions, with their performance heavily contingent on user-defined parameters. Correlation-based methods [22]–[24], seek to determine seismic events by correlating waveforms across receivers, offering enhanced noise resilience and improving consistency across multiple sites. These methods signify a departure from the reliance on energy metrics, aligning detection with waveform correlation. Akaike Information Criterion (AIC)-based methods [25]–[28] distinguish themselves by their capacity to identify the global minimum AIC value without an exclusive dependence on amplitude thresholds or waveform similarity. This attribute is particularly advantageous under challenging signal-to-noise ratios, as the AIC method pivots on statistical feature variations [29]. Nevertheless, the computational demand of AIC-based methods is non-negligible [28], and they require additional localization and calibration to ensure the accuracy of first-break picking [30].

Recently, the combination of deep learning and first-break

This work is supported by Key technologies for coordination and interoperation of power distribution service resource under Grant 2021YFB2401300, National Natural Science Foundation of China under Grant 12371512, Science & Technology Research and Development Project of CNPC under Grant 2021ZG03. (*Corresponding author: Jiangshe Zhang, Chunxia Zhang*).

Haowen Bai, Zixiang Zhao, Jiangshe Zhang, Yukun Cui, Chunxia Zhang are with the School of Mathematics and Statistics, Xi'an Jiaotong University, Xi'an, Shaanxi 710049, China (E-mail: {hwbaii, zixiangzhao, cuiyukun}@stu.xjtu.edu.cn, {jszhang, cxzhang}@mail.xjtu.edu.cn).

Zhenbo Guo is with the Geophysical Technology Research Center of Bureau of Geophysical Prospecting, Zhuozhou, Hebei, 072751, P.R.China (E-mail: guozhenbo01@cnpc.com.cn).

Yongjun Wang is with School of Artificial Intelligence, Wenzhou Polytechnic, Wenzhou, Zhejiang, China (E-mail: wangyjmcvti@qq.com).

picking has revolutionized the field of seismology [31]–[36], where neural networks are capable of extracting and interpreting complex features of seismic data, achieving efficient and highly accurate identification of first-break of seismic signals. Deep learning-based automatic picking methods are categorized into single-trace processing methods [37]–[39] and multi-trace processing methods [40]–[43]. Single-trace processing methods employ a strategy of extracting signals from individual traces near the sampling point and use the classification outcomes to ascertain the presence of a first-break at the center of the region. Within this domain, AENet [39] leverages convolutional neural networks (CNNs) with DBSCAN clustering analysis to retrieve the precise first-break. Conversely, multi-trace processing methods process the time-series signals from contiguous receivers into 2-D representations for collective analysis [44], [45]. These methods, such as UNet [40], SegNet [46], ResUnet [47], MSNet [42], evaluate each sampling point within the context of its neighbors, thereby harnessing the spatial correlation inherent between adjacent traces [48]–[52]. This approach tends to yield more reliable outcomes compared to single-trace picking methodologies. The adoption of deep learning for automatic first-break picking augments both the accuracy and efficiency of seismic data analysis. This advancement underscores the transformative potential of seismic detection, resource exploration, and broader geophysical research.

Despite these advances, there are still challenges in deep learning-based first-break picking methods. The production of a substantial and accurately labeled training dataset is a pivotal requirement for the effective training of neural networks. Unfortunately, the construction of such datasets inevitably results in outlier samples and mislabeling, particularly in situations with large volumes of seismic data and intensive manual labor [8], [53]. Outlier samples, although accurate, are like mislabeled data in that their extreme values can seriously impair the model’s learning process and accuracy. The detrimental impact of outlier samples and label noise in the data on the performance of neural networks can be overwhelming, with numerous studies endeavoring to devise strategies that mitigate these effects and enable learning from noisy labels [54]. Approaches such as directed graphical models [55], robust loss functions [56], conditional random fields (CRFs) [57], knowledge graphs [58], and neural networks [59], [60] have been employed to address label noise. These methods are particularly effective at the image level. This challenge also extends to pixel-level labels [61] and textual data [62]. In this paper, we propose an innovative first-break picking algorithm capable of identifying outliers or noisy labels in the data. We model true first-break as latent variables within a probabilistic framework. This shifts our neural network’s focus from mere manual picking to dynamically refined, potential true first-break through iterative updates. This method mirrors strategies previously employed in seismic data analysis. Specifically, it uses auxiliary variables in Full Waveform Inversion (FWI) [63]–[65] to broaden the search space for viable solutions and divide the objective function into several sub-tasks. These sub-tasks are iteratively optimized, enhancing the model’s resilience and adaptability. Similarly, Seismic Blind High-Resolution Inversion (BHRI) uses auxiliary variables to reduce

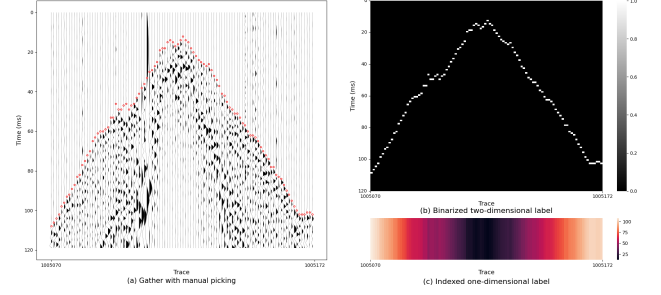


Fig. 1. (a) Amplitude signals. Manual picking are marked with red circles. (b) Binarized 2-D label, the position of the first-break is 1 and the rest is 0. (c) Indexed 1-D label, the index of the first-break among all the sampling points.

dependence on initial estimates [66]. Furthermore, modeling uncertainties in deep learning forecasts with slack variables introduces these uncertainties as soft constraints in the FWI paradigm [67]. This highlights the synergy between traditional seismic imaging methods and deep neural networks’ pattern recognition capabilities. By modeling the true first-break as latent variables and continuously updating them, our approach not only mitigates the influence of outlier data on the learning trajectory but also corrects mislabeling through a systematic refinement process.

Our main contributions are briefly summarized as follows:

- (1) We propose an automatic picking method capable of mining the distribution of first-break. By constructing a probabilistic model that includes potential first-break, our method resists the effects of outlier samples and mislabeling, thereby significantly improving picking accuracy.
- (2) The developed probabilistic model features two inference methods, capable of performing automatic first-break picking and correcting potential errors in manual picking, respectively.
- (3) Extensive experiments containing picking experiments, generalization experiments, noisy signal experiments, and noisy labeling experiments demonstrate the excellent performance of our method. In addition, the proposed algorithm is not limited to a specific network structure and can be generalized to arbitrary neural networks.

The arrangement of the subsequent paper is as follows, in Sec. II, we describe the training process and the inference methodology of the proposed algorithm, with extensive experiments in Sec. III. Conclusions are stated in Sec. IV.

II. METHOD

Before describing the method, we need to unify the notations. In this paper, we adopt multi-trace processing for first-break picking. $x \in R^{M \times N}$ is the amplitude data received at the signal detection point, where N and M represent the number of traces and sampling points in each trace, respectively. Two forms of first-break labels are used in our analysis, as illustrated in Fig. 1. One is an indexed one-dimensional label, denoted by $t \in R^{1 \times N}$. t_k , a number, represents the index of the first-break of k th trace among all the sampling points, as shown in Fig. 1 (c). $y \in R^{M \times N}$ denotes the binarized 2-D label, where k th trace’s label y_k is vectorized to match the size of its corresponding signal vector. The position of the first-break

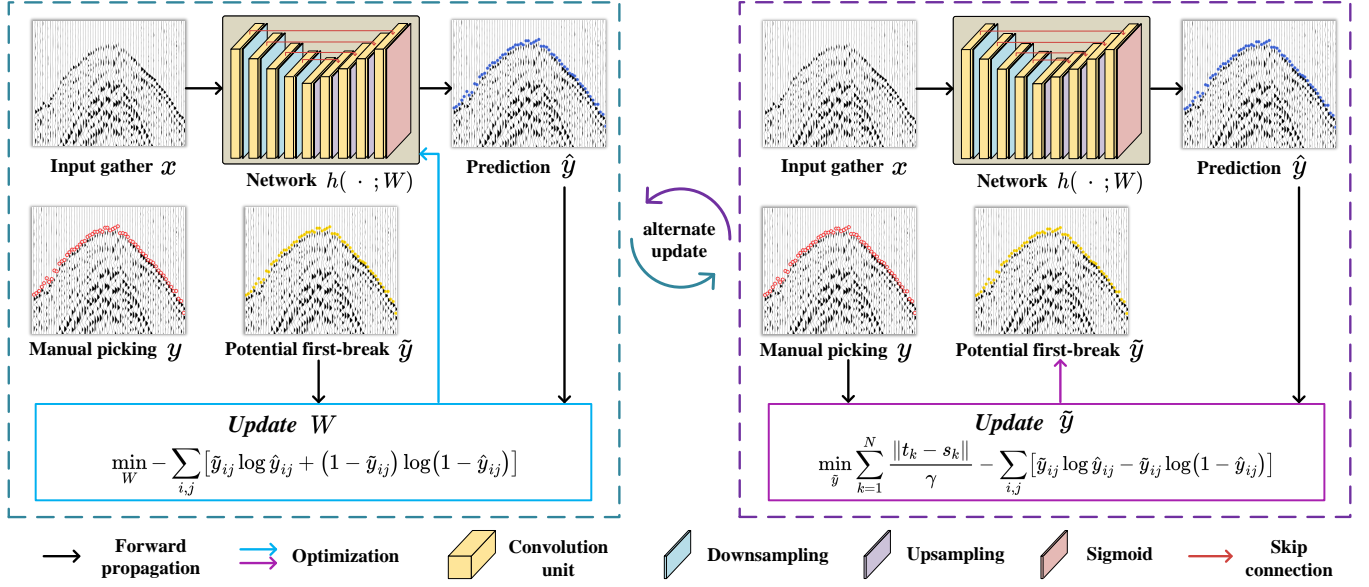


Fig. 2. The training process of SPR. The network parameters W and potential first-break \tilde{y} are alternately updated to simultaneously learn picking as well as manually picking refinement.

is marked as 1, and the remaining elements are set to 0, as shown in Fig. 1 (b). These two forms of labels are inherently interconvertible and maintain a direct correspondence with each other. In the rest of this paper, they will be referred to as the 1-D label t and the 2-D label y to streamline the discussion and analysis.

A. Probabilistic Model

In classification problems, the training objective of the model is usually to maximize the likelihood function:

$$\max_W \mathcal{L}(W) = P(y | x; W), \quad (1)$$

where y , x , and W are the labels, input gathers, and the model parameters, respectively. The same is true for many semantic segmentation-based picking methods. However, due to a variety of factors, some outlier samples or even mislabeling are inevitable, which can seriously affect the training process of neural networks. In this work, we introduce a latent first-break \tilde{y} , which is different from manual picking in some traces. \tilde{y} accounts for outlier sample substitution and mislabeling correction, enhancing modeling quality and reliability. The model is optimized by maximizing the likelihood of the manual picking y and the potential first-break \tilde{y} as follows

$$\begin{aligned} \max_{\tilde{y}; W} \mathcal{L}(\tilde{y}; W) &= P(y, \tilde{y} | x; W) \\ &= P(y | \tilde{y}, x; W) P(\tilde{y} | x; W) \\ &= P(y | \tilde{y}) P(\tilde{y} | x; W). \end{aligned} \quad (2)$$

In the equation above, the first term represents a prior probability model for first-break point labeling. This term calculates the probability of a point being labeled as y given the potential first-break \tilde{y} . We postulate that the probability of mislabeling is independent of the input x and inherently unrelated to the network parameters W . Thus, we simplify the

first term to $P(y | \tilde{y})$, reinforcing our model's assumptions and its structural integrity. The latter item takes \tilde{y} as the prediction target of the network.

Labeling misalignments and outlier samples are sparse, occurring in only a small number of traces. Thus, the Laplace distribution, known for its peaked and heavy-tailed nature, is better suited to capturing the distribution of sparse data. We use the Laplace distribution to model the first-break labeling prior model, i.e.

$$P(y | \tilde{y}) \propto \prod_{k=1}^N \exp\left(-\frac{\|t_k - s_k\|}{\gamma}\right), \quad (3)$$

where s is the 1-D labeling of \tilde{y} as previously described. t_k and s_k are the positions of the manual picking and potential first-break of the k th trace, respectively. γ represents the sensitivity parameter that controls labeling bias, with its choice depending on the specific situation. The equation suggests that each trace's first-break labels follow a Laplace distribution centered around their potential true first-break.

For the prediction target, we assume a joint distribution across all samples, with each sample's probability modeled by a binary Bernoulli distribution:

$$\begin{aligned} P(\tilde{y} | x; W) &= \prod_{i,j} P(\tilde{y}_{ij} | x; W) \\ &= \prod_{i,j} (\hat{y}_{ij})^{\tilde{y}_{ij}} (1 - \hat{y}_{ij})^{1 - \tilde{y}_{ij}}, \end{aligned} \quad (4)$$

where $i \in 1, \dots, M$ and $j \in 1, \dots, N$ represent the indices of the sample points in the vertical and horizontal dimensions, respectively. $\hat{y} = h(x; W)$ is the prediction of the network, which we learn with original UNet [68]. The UNet structure used in the training process is illustrated in Fig. 2.

B. Learning and Inference

By taking Eq. (3) and Eq. (4) into Eq. (2) and logging it, we obtain:

$$\log \mathcal{L}(\tilde{y}, W) = - \sum_{k=1}^N \frac{\|t_k - s_k\|}{\gamma} + \sum_{i,j} [\tilde{y}_{ij} \log \hat{y}_{ij} + (1 - \tilde{y}_{ij}) \log(1 - \hat{y}_{ij})]. \quad (5)$$

To maximize the log likelihood function, we minimize its negative, $-\log \mathcal{L}(\tilde{y}, W)$, using the strategy of updating \tilde{y} and W alternately. By fixing \tilde{y} and optimizing W , the optimization is formulated as:

$$\min_W - \sum_{i,j} [\tilde{y}_{ij} \log \hat{y}_{ij} + (1 - \tilde{y}_{ij}) \log(1 - \hat{y}_{ij})]. \quad (6)$$

This is the binary cross-entropy function, which is often used in training networks for binary classification problems. The above equation means that we train the network with the current potential first-break \tilde{y} as the label. Note that our network learns the potential first-break \tilde{y} instead of the manual picking y . The update of \tilde{y} is obtained through the following optimization:

$$\min_{\tilde{y}} \sum_{k=1}^N \frac{\|t_k - s_k\|}{\gamma} - \sum_{i,j} [\tilde{y}_{ij} \log \hat{y}_{ij} - \tilde{y}_{ij} \log(1 - \hat{y}_{ij})]. \quad (7)$$

Here, \tilde{y} and s represent different forms of the same variable, making their optimization equivalent. The equation implies that updating \tilde{y} must align with the current network output and the artificial label y . The alternating updates of \tilde{y} and W ensure the maximization of Eq. (5). The complete training process of SPR is shown in Algorithm 1.

The trained model can perform inference in two ways: in the absence of y , it predicts the point of the first-break using a model trained to predict the potential true first-break more accurately than manual labeling. The prediction is as follows:

$$y^* = \arg \max_{\tilde{y}} P(\tilde{y} | x; W). \quad (8)$$

On the other hand, if manual picking y is available, we can infer

$$y^{**} = \arg \max_{\tilde{y}} P(y | \tilde{y}) P(\tilde{y} | x; W) \quad (9)$$

to refine manual picking, with y^{**} being the refinement of y . The application of the two inferences is shown in subsequent experiments.

TABLE I

INFORMATION ABOUT THE REAL DATA USED IN THIS PAPER. TO ADAPT THE INPUT AND OUTPUT OF THE NEURAL NETWORK, THE ORIGINAL SIGNAL IS FILLED WITH ZEROS TO BECOME THE INPUT SHAPE.

Data Information					
Dataset	trace num	sample num	sample rate	first-break	input shape
Sudbury [69]	1810220	1001	1 ms	0-92 ms	224×1024
Lalor [69]	2424923	1501	2 ms	0-220 ms	192×1504

Algorithm 1 SPR training Algorithm

Require:

Training set $\{x, y\}$, the number of epochs K .

Ensure:

Network prediction \hat{y} .

- 1: Initialize $W, \tilde{y} = y$. Calculate the number of steps L based on the dataset size.
 - 2: **for** $epoch = 1$ **to** K **do**
 - 3: **for** $step = 1$ **to** L **do**
 - 4: Sample data (x, y) and the corresponding \tilde{y} .
 - 5: Predict \hat{y} using current network parameters W .
 - 6: Update W by Eq. (6).
 - 7: Update \tilde{y} by Eq. (7).
 - 8: **end for**
 - 9: **end for**
-

III. EXPERIMENT

A. Setup

All of our experiments are performed on two publicly available datasets. The Sudbury dataset [69] contains 1,810,220 traces, each containing 1001 sampling points at a sampling rate of 1 ms. The Lalor dataset [69] contains 2,424,923 traces with 1001 sampling points and a sampling rate of 2 ms. Basic details of the datasets are presented in Table I, with further information available in [69]. In adapting to the network structure, the amplitude signal is processed to a size that can accommodate downsampling and upsampling, as shown in the last column of Tab. I, with the expanded region filled by zeros. Both datasets are divided into training set/validation set/test set according to the ratio of 8:1:1 for experimentation. Not all traces in the datasets are manually labeled, hence the picking results of different methods for these traces are omitted from the visualization.

The experiment consists of four parts. The first part, a picking comparison experiment, is conducted on the Sudbury and Lalor datasets to compare the picking performance of different methods. The second part is a generalization experiment, where the models from the first part are directly transferred to assess the algorithm's generalization performance. The third part involves experiments with noisy signals, where Gaussian noise is artificially added to the Sudbury dataset and picking is performed under various noise levels. The last part involves experiments with noisy labels, conducted on the Sudbury dataset. In the first three parts, the experimental results are inferred solely based on Eq. (8). For the experiments with noisy labels, we apply Eq. (8) on the test set to verify the ability to learn from noisy labels, and also apply Eq. (9) on its training set to confirm the capability to refine manual picking.

The comparison methods in the experiments are comprised of the following state-of-the-art deep learning-based picking methods: UNet [40], AENet [39], SegNet [46], ResUNet [47] and MSNet [42]. The batch size, learning rate and optimizer are set to 8, 1e-4 and Adam, respectively. Parameter γ is set to 5 to balance network output and refinement performance. The compared methods retain their original structures and are retrained using the same training settings employed for our

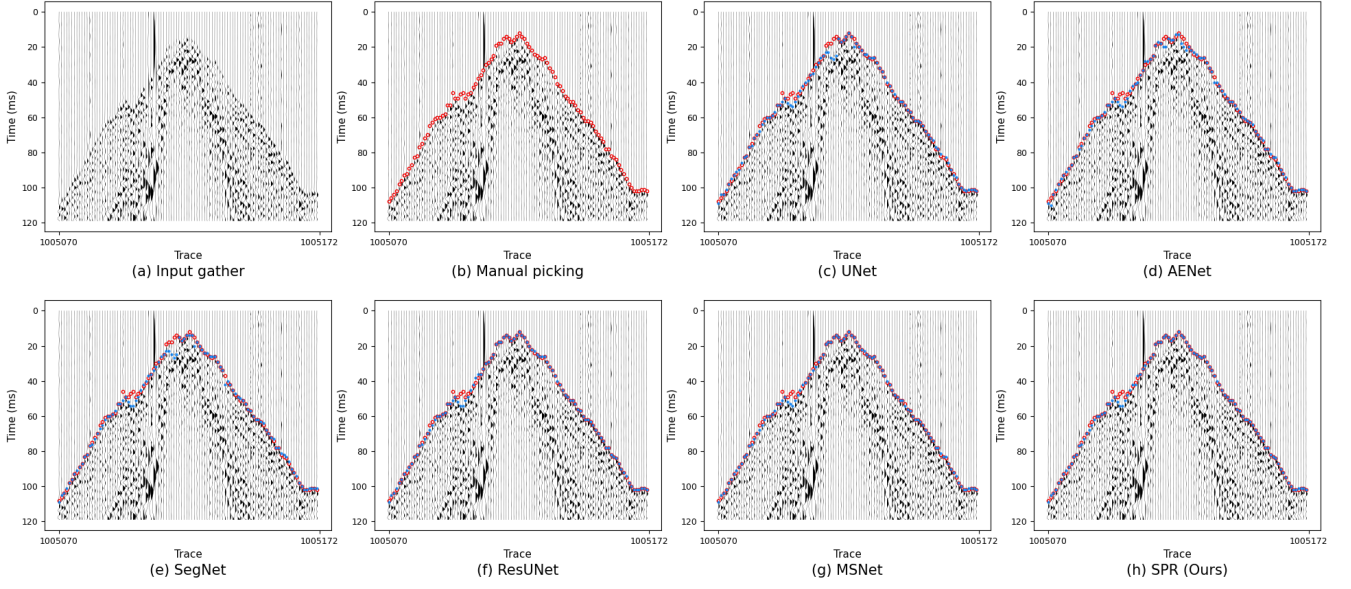


Fig. 3. Comparison of picking results of different methods for trace 1005070-1005172 of dataset Sudbury. Manual picking and picking results of different methods are indicated by red circles and blue dots, respectively.

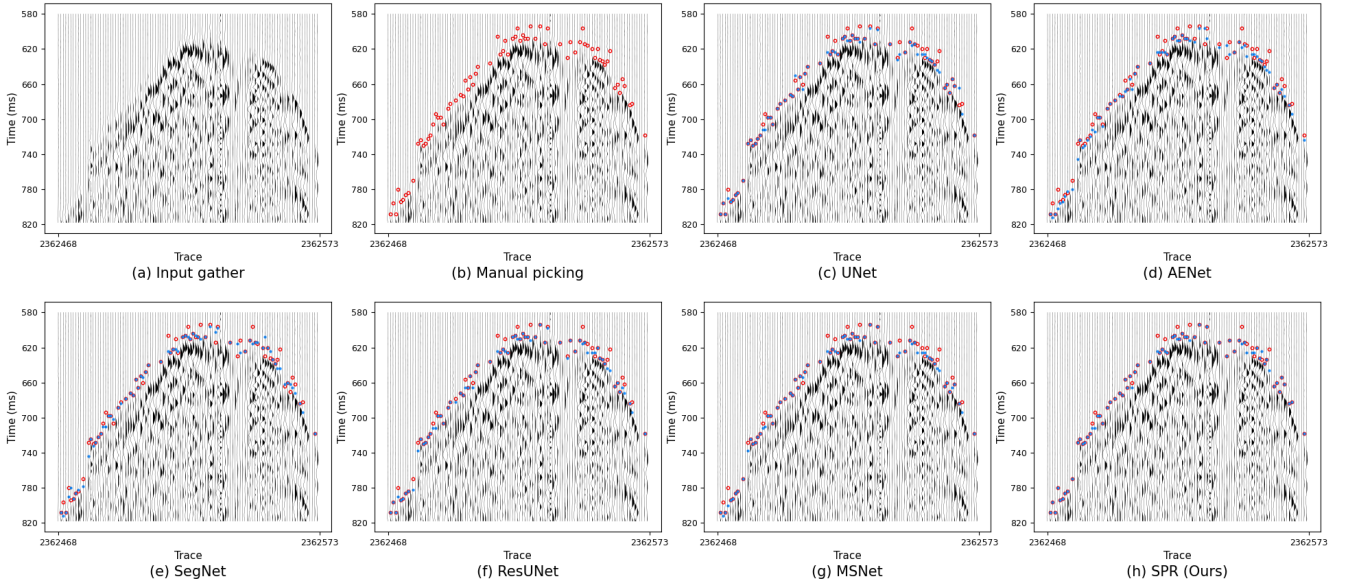


Fig. 4. Comparison of picking results of different methods for trace 2362428-2362573 of dataset Lalor. Manual picking and picking results of different methods are indicated by red circles and blue dots, respectively.

SPR method. All models are trained for 100 epochs on a PC equipped with a single NVIDIA GeForce RTX 3090 GPU.

B. Evaluation

Two metrics are used to verify the accuracy and reliability of our method. We transform the prediction result y^* into 1-D form t^* and use the 1-D manual picking t as a reference. The first evaluation metric is hit rate (HR) [69], which is defined as follows:

$$HR_\delta = \frac{1}{N} \sum_{k=1}^N I(|t_k - t_k^*| \leq \delta), \quad (10)$$

where N is the total number of channels, I is the indicator function, and δ is the error parameter. HR reflects the proportion of correctly identified microseismic wave first-break out of all the potential seismic events present in a dataset. A high HR indicates a strong ability of the algorithm to accurately detect the first-break, which is crucial for subsequent seismic data processing tasks such as travel-time analysis. Additionally, the HR is instrumental in assessing the robustness of a picking method against various challenges, including noise levels, signal distortions, and variations in seismic wave characteristics. In this paper, we compare the performance of the algorithms at $\delta = \{0, 1, 2, 3, 5\}$.

The second metric is the mean absolute error (MAE), which

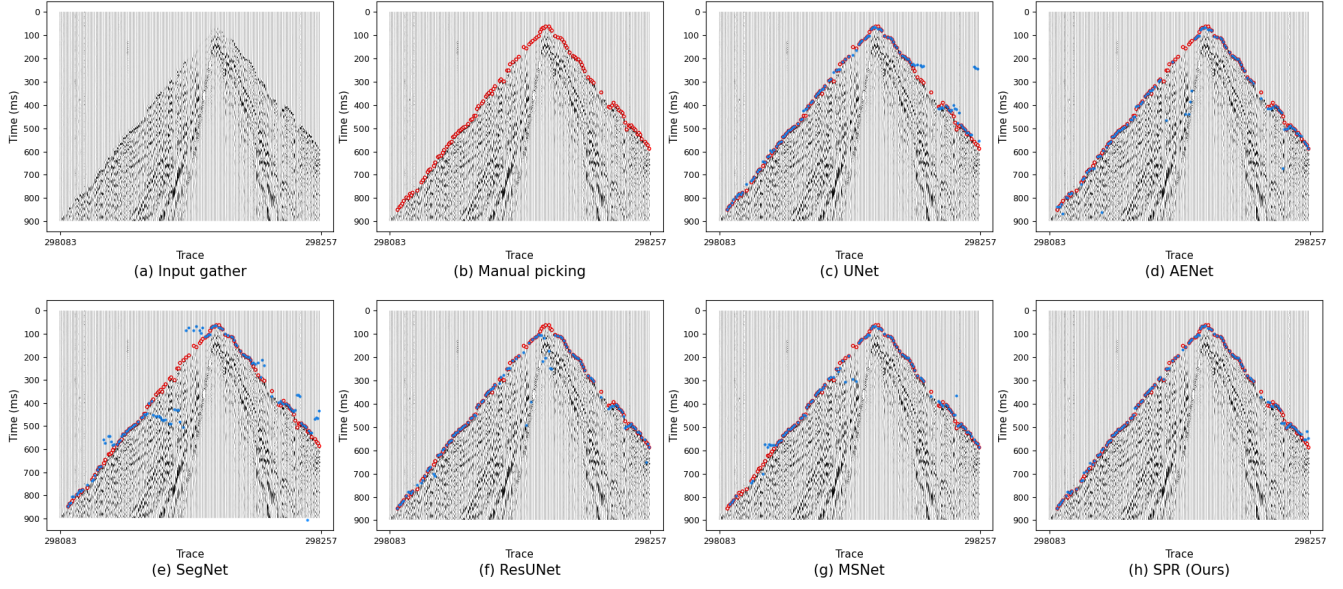


Fig. 5. Generalization experiments for first-break picking. The model is trained on data Sudbury and tested on data Lalor. The figure shows traces 298083-298257 in data Lalor. Manual picking and generalization results of different methods are indicated by red circles and blue dots, respectively.

quantifies the average absolute difference between automatic picking and manual picking. MAE provides a clear and interpretable measure of the average error magnitude, and it is highly resistant to outliers. MAE is defined as:

$$MAE = \frac{1}{N} \sum_{k=1}^N |t_k - t_k^*|. \quad (11)$$

In the noisy label refining experiments, performance evaluation follows the same methodology as in picking performance. However, t^* is replaced with t^{**} , which is derived from y^{**} .

TABLE II

PICKING EXPERIMENTS FOR FIRST-BREAK PICKING. **BOLDFACE** AND UNDERLINE SHOW THE BEST AND SECOND BEST VALUES, RESPECTIVELY.

Dataset: Sudbury						
Method	HR_0	HR_1	HR_2	HR_3	HR_5	MAE
UNet [40]	65.31	89.10	91.56	93.06	94.91	2.6465
AENet [39]	58.04	85.33	88.96	90.35	92.89	5.4552
SegNet [46]	64.92	88.84	91.35	92.86	94.68	2.3475
ResUNet [47]	68.11	89.34	91.47	92.86	94.55	3.5663
MSNet [42]	<u>69.03</u>	<u>89.85</u>	<u>92.16</u>	<u>93.59</u>	<u>95.25</u>	<u>2.2113</u>
SPR (Ours)	74.20	90.26	92.35	93.75	95.63	1.6014

Dataset: Lalor						
Method	HR_0	HR_1	HR_2	HR_3	HR_5	MAE
UNet [40]	90.28	92.15	92.80	93.72	95.43	0.5305
AENet [39]	71.97	86.51	88.12	89.50	92.75	1.2198
SegNet [46]	76.98	89.11	90.69	92.09	94.50	0.7988
ResUNet [47]	91.20	92.09	92.72	93.58	95.56	0.5375
MSNet [42]	<u>91.91</u>	<u>92.56</u>	<u>93.10</u>	<u>93.87</u>	95.52	<u>0.5129</u>
SPR (Ours)	92.60	92.80	93.34	94.14	95.76	0.4821

C. Picking Comparison Experiment

We compare the picking performance of SPR and other methods on dataset Sudbury and dataset Lalor and present the quantitative results in Tab. II. Two cases from dataset

Sudbury and dataset Lalor are shown in Fig. 3 and Fig. 4, respectively, where manual picking are represented by red circles and automatic picking are represented by blue dots.

SPR exhibits a higher HR and a lower MSE, in particular, HR_0 is 5% higher than the suboptimal value, suggesting that our method is more accurate and reliable in correctly identifying the first-break. In the visualization results, there are traces for which manual picking positions cannot be identified by all methods, as exemplified by the 40-60 ms interval in Fig. 3. Raw learning of such traces has the potential to degrade the algorithm's performance on general traces. In contrast, SPR's learning targets are not based on manual pickings and are therefore unaffected by outlier samples, ensuring more consistent picking performance across the dataset.

D. Picking Generalization Experiments

TABLE III

GENERALIZATION EXPERIMENTS FOR FIRST-BREAK PICKING. **BOLDFACE** AND UNDERLINE SHOW THE BEST AND SECOND BEST VALUES, RESPECTIVELY.

Method	Training: Sudbury			Test: Lalor		
	HR_0	HR_1	HR_2	HR_3	HR_5	MAE
UNet [40]	36.34	58.83	66.11	71.32	79.02	15.8180
AENet [39]	52.30	70.85	73.41	75.84	<u>81.97</u>	9.2749
SegNet [46]	43.98	63.71	66.18	68.42	73.95	21.1314
ResUNet [47]	<u>56.14</u>	<u>73.80</u>	<u>75.22</u>	<u>77.25</u>	81.95	5.1749
MSNet [42]	54.00	72.06	74.36	76.66	81.88	14.7028
SPR (Ours)	58.44	76.62	78.90	80.96	85.63	<u>6.2842</u>

Given the variability in seismic data due to geographic location, geological structure, and acquisition techniques, it is crucial for a first-break picking algorithm to demonstrate both efficiency and accuracy under these diverse conditions. To investigate the applicability and robustness of our picking algorithm, as well as its ability to generalize across different

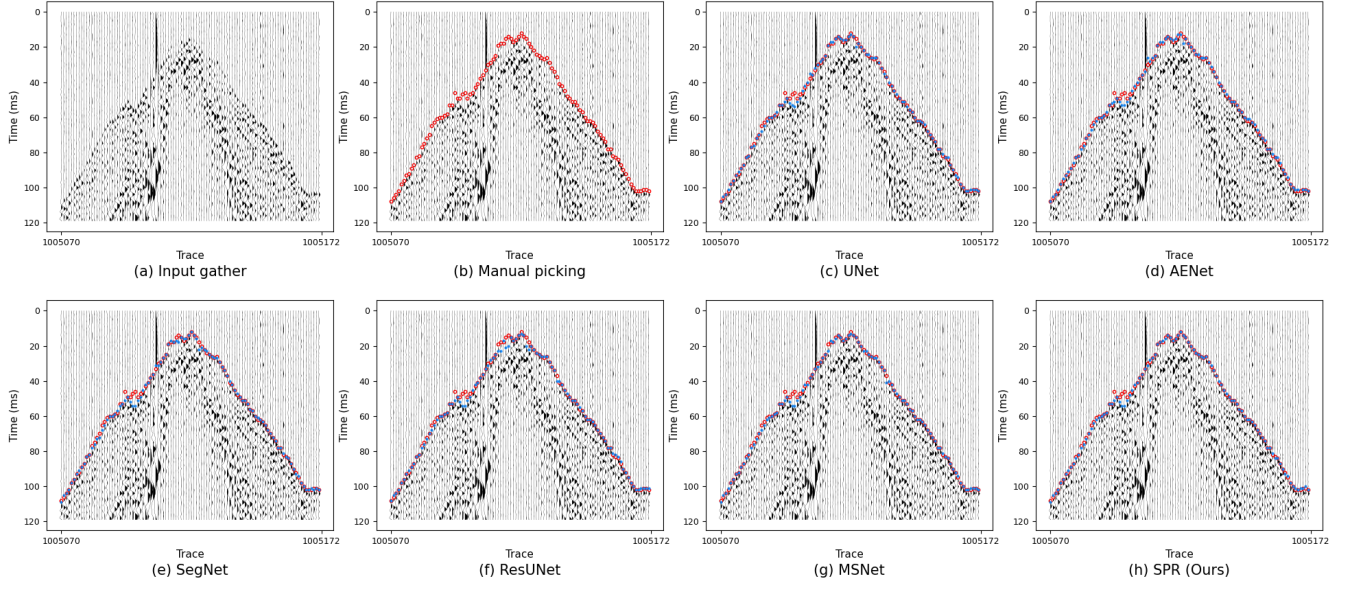


Fig. 6. Comparison of picking results of different methods for trace 1005070-1005172 of dataset Sudbury at noise level 0.05. Manual picking and picking results of different methods are indicated by red circles and blue dots, respectively.

survey sites, we conducted generalization experiments on the Sudbury and Lalor datasets. The rationale behind this setup lies in the significant difference between Sudbury and Lalor datasets, as presented in Table I. Original study [69] also indicates that knowledge generalization between them is quite challenging, making them suitable subjects for a generalization experiment. The models trained on the Sudbury dataset, as described in Sec. III-C are directly tested on the test set of Lalor dataset, and the results of the comparison are displayed in Tab. III and Fig. 5.

The comparison results show that, due to differences in location and sampling rates between the Sudbury (1 ms) and Lalor (2 ms) datasets, the performance of all methods experienced some degradation. However, our method is minimally impacted by these differences and maintained a high degree of consistency with manual picking. SPR demonstrated superior generalization performance compared to other algorithms that learn directly from artificial labels. This suggests that SPR effectively captures the true distribution of the data, thereby avoiding overfitting and enhancing its robustness to various challenges.

E. Noisy Signal Experiment

In this section, Gaussian noise with a mean of 0 is added to the signal to study the noise immunity of the picking method at different noise levels. Following [21], the standard deviation of the Gaussian noise added to each trace is determined by multiplying the trace's maximum raw data amplitude by the noise level (NL). The standard deviation of the noise σ_n in the k -th trace is calculated as follows:

$$\sigma_n = \max(\text{abs}(x_k)) * NL, \quad (12)$$

where x_k is the signal of the k -th trace. We choose three noise levels: 0.05, 0.1, and 0.2, to verify the picking performance on the Sudbury dataset. Comparative results of the same example

in Sec. III-C at different noise levels are shown in Fig. 6, Fig. 7, and Fig. 8. With increasing noise levels, the amplitude signal is gradually drowned out by noise, and all methods are affected to varying degrees. Compared to the other methods, SPR is still able to obtain less biased picking results under strong noise conditions. The quantitative results in Table IV demonstrate that our method has the highest HR and lowest MAE at all noise levels, showcasing the great robustness of SPR in heavily noisy environments.

TABLE IV
NOISY SIGNAL EXPERIMENTS FOR FIRST-BREAK PICKING. **BOLDFACE** AND UNDERLINE SHOW THE BEST AND SECOND BEST VALUES, RESPECTIVELY.

Dataset: Sudbury		Noise Level = 0.05				
Method	HR_0	HR_1	HR_2	HR_3	HR_5	MAE
UNet [40]	60.45	87.46	90.20	91.87	93.97	4.9023
AENet [39]	54.79	83.39	87.16	89.00	91.05	9.3147
SegNet [46]	60.44	87.45	<u>90.78</u>	<u>92.65</u>	<u>94.95</u>	<u>1.9859</u>
ResUNet [47]	62.18	87.77	90.66	92.20	94.20	2.9811
MSNet [42]	<u>62.48</u>	87.51	90.52	92.25	94.29	3.5436
SPR (Ours)	65.43	88.68	91.67	93.41	95.39	1.7251
Dataset: Sudbury		Noise Level = 0.1				
Method	HR_0	HR_1	HR_2	HR_3	HR_5	MAE
UNet [40]	57.49	85.86	90.02	91.96	94.41	2.5230
AENet [39]	47.77	79.87	85.16	87.64	90.24	10.1634
SegNet [46]	53.39	84.16	88.91	91.00	93.51	3.1368
ResUNet [47]	58.06	<u>86.40</u>	<u>90.17</u>	92.06	94.27	2.8152
MSNet [42]	<u>58.13</u>	86.30	90.14	<u>92.16</u>	<u>94.41</u>	<u>2.4048</u>
SPR (Ours)	59.71	87.20	91.14	93.11	95.25	1.8380
Dataset: Sudbury		Noise Level = 0.2				
Method	HR_0	HR_1	HR_2	HR_3	HR_5	MAE
UNet [40]	46.45	78.95	84.67	87.55	90.95	4.5489
AENet [39]	37.68	69.30	76.67	80.04	84.03	11.1791
SegNet [46]	44.79	77.55	84.43	87.46	91.07	3.7183
ResUNet [47]	46.66	<u>79.84</u>	85.59	88.28	<u>91.65</u>	3.7779
MSNet [42]	<u>47.53</u>	79.53	85.70	88.38	91.65	<u>3.7066</u>
SPR (Ours)	50.06	83.07	88.81	91.64	94.67	1.9638

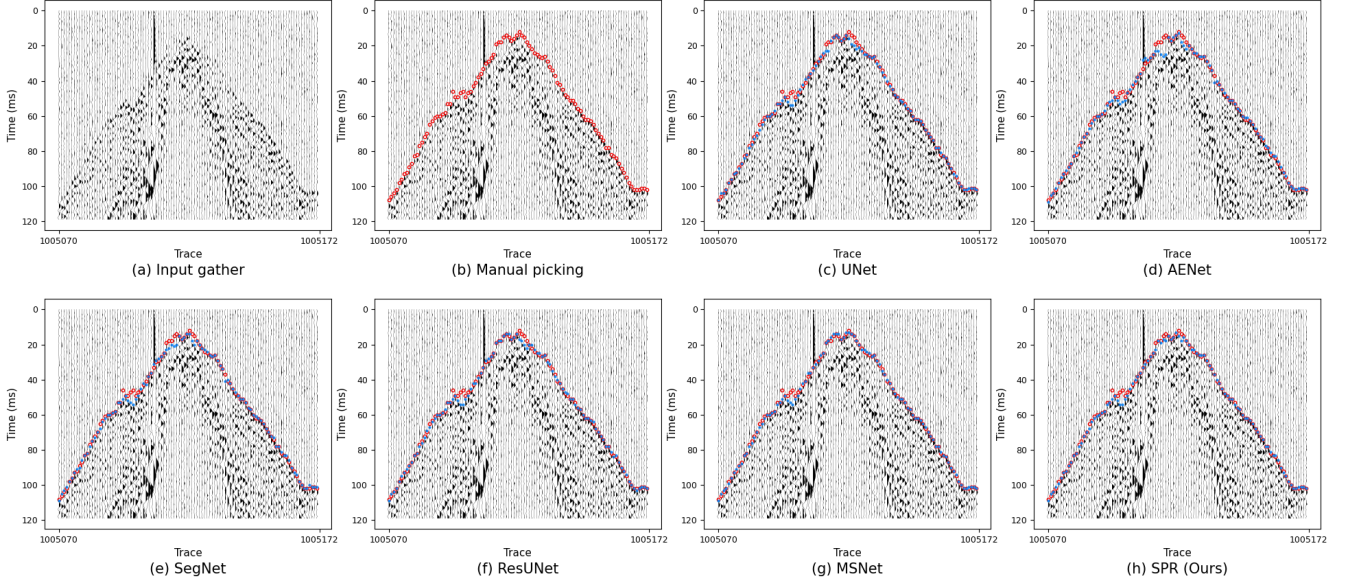


Fig. 7. Comparison of picking results of different methods for trace 1005070-1005172 of dataset Sudbury at noise level 0.1. Manual picking and picking results of different methods are indicated by red circles and blue dots, respectively.

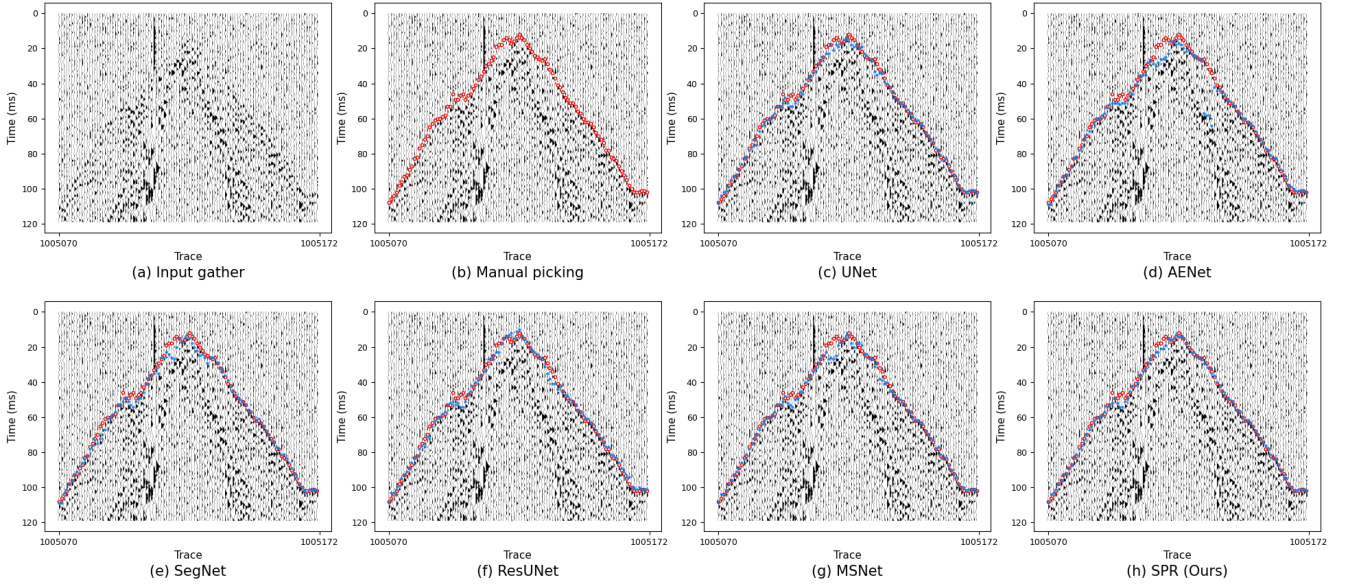


Fig. 8. Comparison of picking results of different methods for trace 1005070-1005172 of dataset Sudbury at noise level 0.2. Manual picking and picking results of different methods are indicated by red circles and blue dots, respectively.

F. Noisy Label Experiment

What distinguishes our approach from others is the ability to learn correctly from undesirable labeled data. The labeling of the original data is always considered clean and correct. In this section, we add labeling noise to all the training set labels of the Sudbury dataset to validate the automatic picking method's performance in learning from noisily labeled data. We model the distribution of mislabeling for each trace with a Gaussian distribution, the noisy labels are calculated as follows,

$$\tilde{t}_k = t_k + \epsilon, \quad (13)$$

where t_k is the indexed manual picking of the k -th trace, \tilde{t}_k is the noisy labeling after noise addition, ϵ is Gaussian noise

with mean 0 and variance 3. The addition of noise causes the first-break label of the training set to be shifted around the time dimension, and the noisy labels are marked with green circles in Fig. 9. The first row of Table V reveals the deviation between the noisy labels and the original manual picking, showing an average deviation of 2.4 sampling points. Only 13.30% of the labels remain in their original positions, indicating significant displacement for the majority.

The training set accompanied by noisy labels is used to train the neural network. For SPR, we utilized artificial labels and employed the results of Eq. (9) as the refined labels. For the other compared methods, we directly use their output as the refinement results. The results of the label refinement are

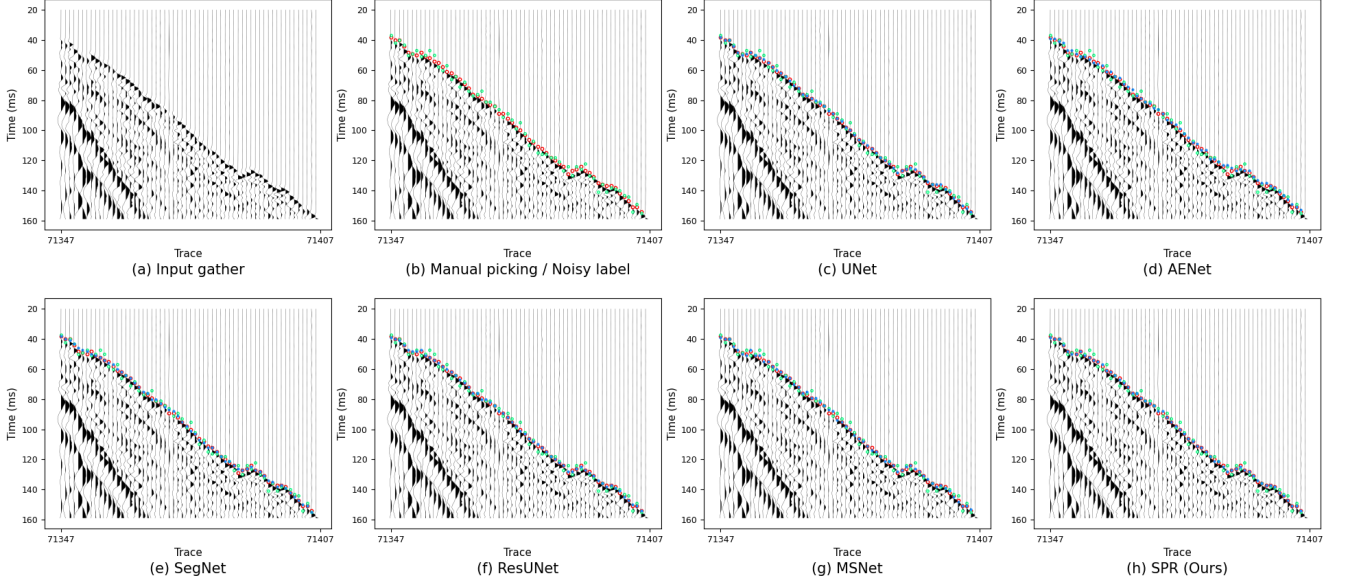


Fig. 9. Comparison of noisy label refinement of different methods for trace 71347-71407 of dataset Sudbury. Manual picking and picking results of different methods are indicated by red circles and blue dots, respectively. Noisy labels are indicated by green circles.

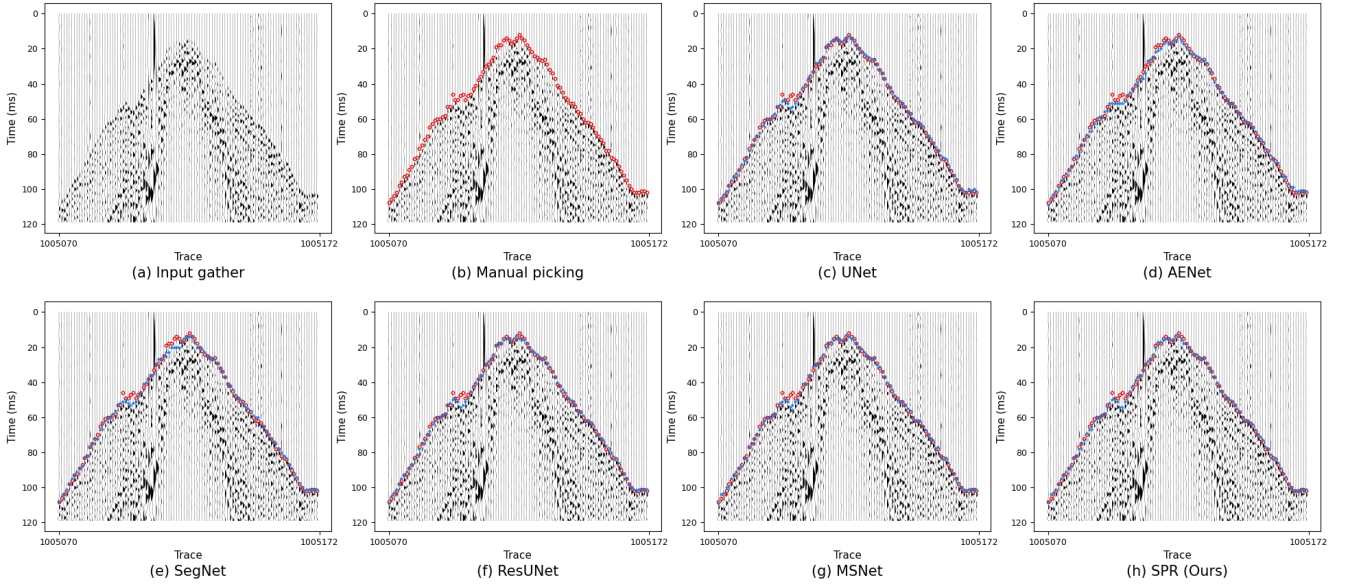


Fig. 10. Comparison of noisy label picking of different methods for trace 1005070-1005172 of dataset Sudbury. Manual picking and picking results of different methods are indicated by red circles and blue dots, respectively.

displayed in Tab. V and Fig. 9. Due to the degradation of label quality, no method other than SPR is able to achieve effective picking. SPR withstands the noise and can successfully improve the HR_0 of label refinement to 56.24%, nearly 10% higher than the suboptimal value, despite only 13.30% of the labels being in the correct position. Furthermore, our method uniquely refines MAE below that of the noisy labels, indicating strong tolerance to label noise. In contrast, other methods show more biased refinement results influenced by the noisy labels. The visualization in Fig. 9 also demonstrates that our refinement results are more consistent with the true first-break whereas other methods fail to obtain satisfactory results.

Second, the model trained on the training set with noisy

labels is applied to the test set of the Sudbury dataset to verify the picking performance. Manual picking on the test set is only used to verify picking accuracy, therefore, the green circles with noise labels are not represented in Fig. 10. The samples selected remain the same as in Sections III-C and III-E. It is evident that the picking performance of the compared methods, as shown in the middle of Fig. 10, is significantly impaired by the presence of noise in the labels, whereas our method continues to guarantee excellent picking results. Quantitative comparisons, as shown in Tab. V, reveal that our method achieves superior HR across all δ values, along with the lowest MAE. This success is attributed to our modeling and learning strategy for the potential first-break.

TABLE V
PERFORMANCE OF NOISY LABELS EXPERIMENTS. **BOLDFACE** AND UNDERLINE SHOW THE BEST AND SECOND BEST VALUES, RESPECTIVELY.

Label Refinement Performance of Noisy Label Experiments						
Methods	HR_0	HR_1	HR_2	HR_3	HR_5	MAE
Noisy Label	13.30	38.35	59.44	75.62	93.31	2.4134
UNet [40]	43.97	83.59	90.18	92.41	94.26	3.3341
AENet [39]	28.42	67.94	82.66	87.36	90.41	9.8110
SegNet [46]	42.49	83.22	90.92	92.23	<u>95.29</u>	2.8869
ResUNet [47]	<u>46.79</u>	<u>85.15</u>	90.78	92.76	<u>94.53</u>	3.0953
MSNet [42]	43.55	84.84	<u>91.54</u>	93.41	95.01	<u>2.8739</u>
SPR (Ours)	56.24	88.75	92.60	94.20	95.79	1.7347

Picking Performance of Noisy Label Experiments						
Methods	HR_0	HR_1	HR_2	HR_3	HR_5	MAE
UNet [40]	44.53	83.47	90.95	93.22	95.10	2.6880
AENet [39]	28.59	68.40	83.34	88.18	91.35	9.1939
SegNet [46]	42.76	82.94	90.71	93.24	95.18	2.3577
ResUNet [47]	45.10	<u>84.64</u>	91.48	93.65	<u>95.36</u>	2.4516
MSNet [42]	45.29	84.53	<u>91.59</u>	93.68	95.23	<u>2.3580</u>
SPR (Ours)	55.97	88.45	92.26	93.92	95.61	2.0987

TABLE VI
PARAMETER INVESTIGATION FOR FIRST-BREAK PICKING. **BOLDFACE** SHOWS THE BEST VALUES.

Parameter Investigation: Picking Experiments						
γ	HR_0	HR_1	HR_2	HR_3	HR_5	MAE
500	55.11	79.69	85.43	87.63	93.57	6.4912
50	60.18	84.61	88.19	89.16	93.99	5.1945
5	74.20	90.26	92.35	93.75	<u>95.63</u>	1.6014
0.5	<u>73.26</u>	90.18	<u>92.30</u>	93.74	95.64	1.7769
0.05	67.22	89.53	91.41	93.28	95.39	2.3342

Parameter Investigation: Noisy Label Refinement						
γ	HR_0	HR_1	HR_2	HR_3	HR_5	MAE
500	40.69	79.49	87.95	90.33	91.19	5.9617
50	44.69	83.13	90.25	92.56	92.68	4.6519
5	56.24	88.75	92.60	94.20	95.79	1.7347
0.5	<u>50.26</u>	86.99	<u>92.02</u>	<u>94.13</u>	<u>95.51</u>	2.8361
0.05	46.83	85.24	91.89	93.96	95.49	2.9477

Parameter Investigation: Noisy Label Picking						
γ	HR_0	HR_1	HR_2	HR_3	HR_5	MAE
500	25.97	60.19	75.49	83.49	90.12	9.3734
50	40.26	75.18	83.94	88.64	89.17	7.1682
5	55.97	88.45	92.26	93.92	95.61	2.0987
0.5	<u>54.68</u>	<u>87.49</u>	<u>91.98</u>	<u>93.81</u>	<u>95.32</u>	<u>2.1653</u>
0.05	44.85	84.99	91.46	93.70	95.33	2.4397

G. Parameter Investigation

In this section, we investigate the impact of parameter γ on the performance. Picking experiments and experiments with noisy labels are performed on the Sudbury dataset for different γ values, while the rest of the training setup parameters remain unchanged. The results of the investigation are displayed in Tab. VI.

When γ is too small, the first term in Eq. (7) dominates, and the optimization result of \tilde{y} is highly consistent with y . Therefore, the algorithm will gradually degenerate into an algorithm with manual picking as the learning objective, losing the ability to mine potential first-break. Consequently, there is a slight decrease in both the picking and correcting abilities, as

shown in Tab. VI. When γ is too large, the network's learning target heavily relies on updating \tilde{y} in the early training stages, which impacts the training outcomes and proves even less effective than directly learning manual picking. Therefore, in this paper, we choose $\gamma = 5$ to balance the learning of the network as well as the mining of potential first-break.

IV. DISCUSSION AND CONCLUSION

A. Discussion

In our formulation of Eq. (2), we posit that the manual labeling y is independent of x given the true first-break \tilde{y} , allowing for the simplification of $P(y | \tilde{y}, x; W)$ to $P(y | \tilde{y})$. This assumption is premised on the notion that errors in manual labeling are predominantly influenced by incomplete accuracy of the labeling (imprecision around the true first-break point) rather than by errors arising from external factors like a lack of expertise (marking one period too early or too late), differing annotation standards (choosing among peaks, troughs, or onset points), or the characteristics of x itself. This modeling strategy also effectively separates the network's predictive terms from the prior labeling terms within the likelihood function, streamlining both analysis and computation.

The Laplace distribution, chosen for its sharp peak and ease of computation, particularly in log-likelihood calculations, is apt for modeling labeling errors due to its higher probability density near zero compared to Gaussian and t -distributions. Its frequent application in prior distribution modeling further motivated its selection in our study for capturing potential labeling inaccuracies.

However, the efficacy of the Laplace distribution heavily depends on the scale parameter. Our approach employs the strategy of a uniform scale parameter. This strategy simplifies the model but it overlooks variability in sample sizes and unknown standard deviations, which can be addressed more effectively by more flexible distributions like the t -distribution. This limitation suggests that for more complex signal types or more diverse error sources, a uniform scale parameter may not be universally optimal. Moreover, the fixed statistical properties of the Laplace distribution, such as its skewness and kurtosis, could restrict its applicability in situations demanding greater statistical flexibility.

Looking ahead, we aim to explore more adaptable statistical models, including the t -distribution and asymmetric distributions, which offer better accommodation for varied sample sizes and complex signal characteristics. Additionally, we plan to investigate the potential benefits of modeling $P(y | \tilde{y}, x; W)$ in relation to x , to enhance our model's adaptability to the complex scenarios presented by x . This future work will strive to address the limitations identified and to refine our approach for even more accurate and flexible seismic data analysis.

B. Conclusion

In this article, we propose a novel first-break picking algorithm targeting challenges posed by outlier samples and noisy labels. Our method constructs a joint probabilistic model that combines manual picking with potential true first-break. These are treated as variables and are alternately optimized

alongside neural network parameters. The core innovation of our algorithm is its dual capability. It can execute first-break picking with enhanced precision and refine the manual picking. This dual functionality is validated by extensive experiments on real seismic data, including comparisons of picking performance, generalization capabilities, and tests on noisy signals and noisy labels. The results consistently underscore the robustness and applicability of our approach in accurately identifying first-break in seismic data. Furthermore, our algorithm provides a modeling approach for first-break picking, applicable to both training and inference, that can be adapted to neural networks of any structure.

REFERENCES

- [1] J. Verdon, J.-M. Kendall, D. White, and D. Angus, "Linking microseismic event observations with geomechanical models to minimise the risks of storing co2 in geological formations," *Earth and Planetary Science Letters*, vol. 305, no. 1-2, pp. 143–152, 2011.
- [2] A. L. Stork, J. P. Verdon, and J.-M. Kendall, "The microseismic response at the in salah carbon capture and storage (ccs) site," *International Journal of Greenhouse Gas Control*, vol. 32, pp. 159–171, 2015.
- [3] D. G. Caglayan, N. Weber, H. U. Heinrichs, J. Linßen, M. Robinus, P. A. Kukla, and D. Stolten, "Technical potential of salt caverns for hydrogen storage in europe," *International Journal of Hydrogen Energy*, vol. 45, no. 11, pp. 6793–6805, 2020.
- [4] J. Mestayer, B. Cox, P. Wills, D. Kiyashchenko, J. Lopez, M. Costello, S. Bourne, G. Ugueto, R. Lupton, G. Solano *et al.*, "Field trials of distributed acoustic sensing for geophysical monitoring," in *Seg technical program expanded abstracts 2011*. Society of Exploration Geophysicists, 2011, pp. 4253–4257.
- [5] E. F. Williams, M. R. Fernández-Ruiz, R. Magalhaes, R. Vanthillo, Z. Zhan, M. González-Herráez, and H. F. Martins, "Distributed sensing of microseisms and teleseisms with submarine dark fibers," *Nature communications*, vol. 10, no. 1, p. 5778, 2019.
- [6] P. R. Stevenson, "Microearthquakes at flathead lake, montana: A study using automatic earthquake processing," *Bulletin of the Seismological Society of America*, vol. 66, no. 1, pp. 61–80, 1976.
- [7] R. V. Allen, "Automatic earthquake recognition and timing from single traces," *Bulletin of the seismological society of America*, vol. 68, no. 5, pp. 1521–1532, 1978.
- [8] Z. Qin, S. Pan, L. Hu, Q. Cui, and Q. Gou, "First-arrival automatic picking based on improved energy ratio method and outlier detection theory," *Acta Geophysica*, vol. 69, no. 5, pp. 1667–1677, 2021.
- [9] R. Allen, "Automatic phase pickers: Their present use and future prospects," *Bulletin of the Seismological Society of America*, vol. 72, no. 6B, pp. S225–S242, 1982.
- [10] M. Baer and U. Kradolfer, "An automatic phase picker for local and teleseismic events," *Bulletin of the Seismological Society of America*, vol. 77, no. 4, pp. 1437–1445, 1987.
- [11] P. S. Earle and P. M. Shearer, "Characterization of global seismograms using an automatic-picking algorithm," *Bulletin of the Seismological Society of America*, vol. 84, no. 2, pp. 366–376, 1994.
- [12] S.-c. Li, S. Cheng, L.-p. Li, S.-s. Shi, and M.-g. Zhang, "Identification and location method of microseismic event based on improved sta/ita algorithm and four-cell-square-array in plane algorithm," *International Journal of Geomechanics*, vol. 19, no. 7, p. 04019067, 2019.
- [13] J. Zhang, Y. Tang, and H. Li, "Sta/ita fractal dimension algorithm of detecting the p-wave arrival," *Bulletin of the Seismological Society of America*, vol. 108, no. 1, pp. 230–237, 2018.
- [14] Z. Chen and R. R. Stewart, "A multi-window algorithm for real-time automatic detection and picking of p-phases of microseismic events," *CREWES Res. Rep.*, vol. 18, pp. 1–9, 2006.
- [15] X. Longjun and C. Yabin, "Easy detection for the high-pass filter cut-off frequency of digital ground motion record based on sta/ita method: A case study in the 2008 wenchuan mainshock," *Journal of Seismology*, vol. 25, no. 5, pp. 1281–1300, 2021.
- [16] Y. Jiang, P. Peng, L. Wang, and Z. He, "Automated locating mining-induced microseismicity without arrival picking by weighted sta/ita traces stacking," *Sustainability*, vol. 12, no. 9, p. 3665, 2020.
- [17] C. Mborah and M. Ge, "Improving the first-arrival picking in mine microseismic data using a stationary discrete wavelet denoising,"
- [18] L. Han, "Microseismic monitoring and hypocenter location," Ph.D. dissertation, University of Calgary, 2010.
- [19] M. Lee, J. Byun, D. Kim, J. Choi, and M. Kim, "Improved modified energy ratio method using a multi-window approach for accurate arrival picking," *Journal of Applied Geophysics*, vol. 139, pp. 117–130, 2017.
- [20] Z. Chen, "A multi-window algorithm for automatic picking of microseismic events on 3-c data," in *SEG International Exposition and Annual Meeting*. SEG, 2005, pp. SEG–2005.
- [21] D. Kim, Y. Joo, and J. Byun, "First-break picking method based on the difference between multiwindow energy ratios," *IEEE Transactions on Geoscience and Remote Sensing*, vol. 61, pp. 1–10, 2023.
- [22] J. B. Molyneux and D. R. Schmitt, "First-break timing; arrival onset times by direct correlation," *Geophysics*, vol. 64, no. 5, pp. 1492–1501, 1999.
- [23] D. Raymer, J. Rutledge, and P. Jaques, "Semiautomated relative picking of microseismic events," in *SEG Technical Program Expanded Abstracts 2008*. Society of Exploration Geophysicists, 2008, pp. 1411–1414.
- [24] M. Senkaya and H. Karsli, "A semi-automatic approach to identify first arrival time: the cross-correlation technique (cct)," *Earth Sciences Research Journal*, vol. 18, no. 2, pp. 107–113, 2014.
- [25] R. Tozzi, F. Masci, and M. Pezzopane, "A stress test to evaluate the usefulness of akaike information criterion in short-term earthquake prediction," *Scientific reports*, vol. 10, no. 1, p. 21153, 2020.
- [26] M. Leonard and B. Kennett, "Multi-component autoregressive techniques for the analysis of seismograms," *Physics of the Earth and Planetary Interiors*, vol. 113, no. 1-4, pp. 247–263, 1999.
- [27] N. Maeda, "A method for reading and checking phase times in autoprocessing system of seismic wave data," *Zisin*, vol. 38, pp. 365–379, 1985.
- [28] Y. Long, J. Lin, B. Li, H. Wang, and Z. Chen, "Fast-aic method for automatic first arrivals picking of microseismic event with multitrace energy stacking envelope summation," *IEEE Geoscience and Remote Sensing Letters*, vol. 17, no. 10, pp. 1832–1836, 2019.
- [29] M. Leonard, "Comparison of manual and automatic onset time picking," *Bulletin of the Seismological Society of America*, vol. 90, no. 6, pp. 1384–1390, 2000.
- [30] C. Mborah and M. Ge, "Enhancing manual p-phase arrival detection and automatic onset time picking in a noisy microseismic data in underground mines," *International Journal of Mining Science and Technology*, vol. 28, no. 4, pp. 691–699, 2018.
- [31] Y. Hollander, A. Merouane, and O. Yilmaz, "Using a deep convolutional neural network to enhance the accuracy of first-break picking," in *SEG International Exposition and Annual Meeting*. SEG, 2018, pp. SEG–2018.
- [32] Y. Chen, G. Zhang, M. Bai, S. Zu, Z. Guan, and M. Zhang, "Automatic waveform classification and arrival picking based on convolutional neural network," *Earth and Space Science*, vol. 6, no. 7, pp. 1244–1261, 2019.
- [33] G. Zhang, C. Lin, and Y. Chen, "Convolutional neural networks for microseismic waveform classification and arrival picking," *Geophysics*, vol. 85, no. 4, pp. WA227–WA240, 2020.
- [34] W. Zhu and G. C. Beroza, "Phasenet: A deep-neural-network-based seismic arrival-time picking method," *Geophysical Journal International*, vol. 216, no. 1, pp. 261–273, 2019.
- [35] S. Han, Y. Liu, Y. Li, and Y. Luo, "First arrival traveltimes picking through 3-d u-net," *IEEE Geoscience and Remote Sensing Letters*, vol. 19, pp. 1–5, 2021.
- [36] K. C. Tsai, W. Hu, X. Wu, J. Chen, and Z. Han, "First-break automatic picking with deep semisupervised learning neural network," in *SEG Technical Program Expanded Abstracts 2018*. Society of Exploration Geophysicists, 2018, pp. 2181–2185.
- [37] M. D. McCormack, D. E. Zaucho, and D. W. Dushek, "First-break refraction event picking and seismic data trace editing using neural networks," *Geophysics*, vol. 58, no. 1, pp. 67–78, 1993.
- [38] X. Qu, G. Yan, D. Zheng, S. Fan, Q. Rao, and J. Jiang, "A deep learning-based automatic first-arrival picking method for ultrasound sound-speed tomography," *IEEE Transactions on Ultrasonics, Ferroelectrics, and Frequency Control*, vol. 68, no. 8, pp. 2675–2686, 2021.
- [39] C. Guo, T. Zhu, Y. Gao, S. Wu, and J. Sun, "Aenet: Automatic picking of p-wave first arrivals using deep learning," *IEEE Transactions on Geoscience and Remote Sensing*, vol. 59, no. 6, pp. 5293–5303, 2020.
- [40] L. Hu, X. Zheng, Y. Duan, X. Yan, Y. Hu, and X. Zhang, "First-arrival picking with a u-net convolutional network," *Geophysics*, vol. 84, no. 6, pp. U45–U57, 2019.
- [41] L. Hu, X. Zheng, and Y. Duan, "U-net convolutional networks for first arrival picking," in *SEG 2018 Workshop: SEG Maximizing Asset Value Through Artificial Intelligence and Machine Learning, Beijing, China*,

- 17-19 September 2018. Society of Exploration Geophysicists and the Chinese Geophysical Society, 2018, pp. 15–18.
- [42] G. Sheng, S. Yang, X.-G. Tang, and X. Guo, “Arrival-time picking of microseismic events based on msnet,” *Geophysics*, vol. 87, no. 2, pp. KS57–KS71, 2022.
- [43] P. Yuan, S. Wang, W. Hu, X. Wu, J. Chen, and H. Van Nguyen, “A robust first-arrival picking workflow using convolutional and recurrent neural networks,” *Geophysics*, vol. 85, no. 5, pp. U109–U119, 2020.
- [44] P. Jiang, F. Deng, X. Wang, P. Shuai, W. Luo, and Y. Tang, “Seismic first break picking through swin transformer feature extraction,” *IEEE Geoscience and Remote Sensing Letters*, vol. 20, pp. 1–5, 2023.
- [45] N. Liu, J. Chen, H. Wu, F. Li, and J. Gao, “Microseismic first-arrival picking using fine-tuning feature pyramid networks,” *IEEE Geosci. Remote. Sens. Lett.*, vol. 19, pp. 1–5, 2022.
- [46] S.-Y. Yuan, Y. Zhao, T. Xie, J. Qi, and S.-X. Wang, “Segnet-based first-break picking via seismic waveform classification directly from shot gathers with sparsely distributed traces,” *Petroleum Science*, vol. 19, no. 1, pp. 162–179, 2022.
- [47] P. Zwartjes and J. Yoo, “First break picking with deep learning—evaluation of network architectures,” *Geophysical Prospecting*, vol. 70, no. 2, pp. 318–342, 2022.
- [48] T. Xie, Y. Zhao, X. Jiao, W. Sang, and S. Yuan, “First-break automatic picking with fully convolutional networks and transfer learning,” in *SEG International Exposition and Annual Meeting*. SEG, 2019, p. D043S152R001.
- [49] J. Zhang and G. Sheng, “First arrival picking of microseismic signals based on nested u-net and wasserstein generative adversarial network,” *Journal of Petroleum Science and Engineering*, vol. 195, p. 107527, 2020.
- [50] S. Yuan, J. Liu, S. Wang, T. Wang, and P. Shi, “Seismic waveform classification and first-break picking using convolution neural networks,” *IEEE Geoscience and Remote Sensing Letters*, vol. 15, no. 2, pp. 272–276, 2018.
- [51] K. Ma, X. Sun, Z. Zhang, J. Hu, and Z. Wang, “Intelligent location of microseismic events based on a fully convolutional neural network (fcnn),” *Rock Mechanics and Rock Engineering*, vol. 55, no. 8, pp. 4801–4817, 2022.
- [52] W. A. Mousa, A. A. Al-Shuhail, and A. Al-Lehyani, “A new technique for first-arrival picking of refracted seismic data based on digital image segmentation,” *Geophysics*, vol. 76, no. 5, pp. V79–V89, 2011.
- [53] Z. Qin, S. Pan, J. Chen, Q. Cui, and J. He, “Method of automatically detecting the abnormal first arrivals using delay time (december 2020),” *IEEE Transactions on Geoscience and Remote Sensing*, vol. 60, pp. 1–8, 2021.
- [54] H. Song, M. Kim, D. Park, and J. Lee, “Learning from noisy labels with deep neural networks: A survey,” *CoRR*, vol. abs/2007.08199, 2020.
- [55] T. Xiao, T. Xia, Y. Yang, C. Huang, and X. Wang, “Learning from massive noisy labeled data for image classification,” in *CVPR*. IEEE Computer Society, 2015, pp. 2691–2699.
- [56] G. Patrini, A. Rozza, A. K. Menon, R. Nock, and L. Qu, “Making deep neural networks robust to label noise: A loss correction approach,” in *CVPR*. IEEE Computer Society, 2017, pp. 2233–2241.
- [57] A. Vahdat, “Toward robustness against label noise in training deep discriminative neural networks,” in *NIPS*, 2017, pp. 5596–5605.
- [58] Y. Li, J. Yang, Y. Song, L. Cao, J. Luo, and L. Li, “Learning from noisy labels with distillation,” in *ICCV*. IEEE Computer Society, 2017, pp. 1928–1936.
- [59] A. Veit, N. Alldrin, G. Chechik, I. Krasin, A. Gupta, and S. J. Belongie, “Learning from noisy large-scale datasets with minimal supervision,” in *CVPR*. IEEE Computer Society, 2017, pp. 6575–6583.
- [60] Y. Wang, W. Liu, X. Ma, J. Bailey, H. Zha, L. Song, and S. Xia, “Iterative learning with open-set noisy labels,” in *CVPR*. Computer Vision Foundation / IEEE Computer Society, 2018, pp. 8688–8696.
- [61] Z. Yu, W. Liu, Y. Zou, C. Feng, S. Ramalingam, B. V. K. V. Kumar, and J. Kautz, “Simultaneous edge alignment and learning,” in *ECCV (3)*, ser. Lecture Notes in Computer Science, vol. 11207. Springer, 2018, pp. 400–417.
- [62] G. Zheng, A. H. Awadallah, and S. T. Dumais, “Meta label correction for noisy label learning,” in *AAAI*. AAAI Press, 2021, pp. 11 053–11 061.
- [63] E. Esser, L. Guasch, T. van Leeuwen, A. Y. Aravkin, and F. J. Herrmann, “Total variation regularization strategies in full-waveform inversion,” *SIAM Journal on Imaging Sciences*, vol. 11, no. 1, pp. 376–406, 2018.
- [64] H. S. Aghamiry, A. Gholami, and S. Operto, “Implementing bound constraints and total-variation regularization in extended full-waveform inversion with the alternating direction method of multiplier: application to large contrast media,” *Geophysical Journal International*, vol. 218, no. 2, pp. 855–872, 04 2019.
- [65] —, “Compound regularization of full-waveform inversion for imaging piecewise media,” *IEEE Transactions on Geoscience and Remote Sensing*, vol. 58, no. 2, pp. 1192–1204, 2020.
- [66] H. Chen, J. Gao, Z. Gao, D. Chen, and T. Yang, “A sequential iterative deep learning seismic blind high-resolution inversion,” *IEEE Journal of Selected Topics in Applied Earth Observations and Remote Sensing*, vol. 14, pp. 7817–7829, 2021.
- [67] A. Siahkoobi, G. Rizzuti, and F. J. Herrmann, *Weak deep priors for seismic imaging*, 2020, pp. 2998–3002.
- [68] O. Ronneberger, P. Fischer, and T. Brox, “U-net: Convolutional networks for biomedical image segmentation,” in *Medical Image Computing and Computer-Assisted Intervention—MICCAI 2015: 18th International Conference, Munich, Germany, October 5-9, 2015, Proceedings, Part III 18*. Springer, 2015, pp. 234–241.
- [69] S. Pierre-Luc, R. Bruno, G. Joumana, N. Jean-Philippe, B. Gilles, and S. Ernst, “A multi-survey dataset and benchmark for first break picking in hard rock seismic exploration,” in *Proc. Neurips 2021 Workshop on Machine Learning for the Physical Sciences (MLAPS)*, 2021.